Group 4 Complexes of Chelating Dianionic [OSO] Binaphtholate Ligands; Synthesis and Alkene Polymerisation Catalysis

Louise S. Natrajan,[a] Claire Wilson,[a] Jun Okuda,[b] and Polly L. Arnold*[a]

Keywords: Binaphthol ligands / Polymerisation catalysis / Organometallic / Group 4 elements / Zirconium / Titanium

Mono- and bis(ligand)titanium and -zirconium complexes of a sulfur-bridged binaphtholate [1,1′-S(2-HOC$_{10}$H$_4$-*t*Bu$_2$-3,6)$_2$] (H$_2$**L**^{SN}) have been synthesised and characterised. Complexes of the general form [M(**L**^{SN})X$_2$] (X = Cl, CH$_2$Ph) are prepared by protonolysis or metathesis. X-ray crystallographic structural characterisation of the dibenzyl complex [Zr(**L**^{SN})(CH$_2$Ph)$_2$] is reported, as well as the structure of its partially oxidised derivative [Zr(**L**^{SN})(CH$_2$Ph)(OCH$_2$Ph)]$_2$. Complexes of the form [M(**L**^{SN})$_2$] are readily formed; these can be converted by comproportionation reactions into the mono-**L**^{SN} derivatives above. The X-ray crystal structure of a bis(sulfur-bridged biphenolate) is presented. The representative complexes have been tested as alkene polymerisation catalysts, in conjunction with a methylalumoxane cocatalyst, and for the first time a zirconium complex of a sulfur-bridged biphenolate-type ligand has been found to be active in the polymerisation of ethene.

1 Introduction

The continuing search for alternatives to cyclopentadienyl-based ancillary ligand sets for Group 4 olefin polymerisation catalysts has produced a huge range of new polydentate ligand systems, of which biphenolates have been identified as good ligands.[1,2] However, aryloxides are not generally considered to contribute sufficient electron density to be isolobal with the cyclopentadienyl ligand.[3] Biphenol ligands in which the two phenol rings are joined in the *ortho* position by a potential donor group, such as sulfur, can provide an increased stabilisation of reactive, electron-deficient metal centres.[4] A diverse range of complexes that contain these atom-bridged biphenolates, where the coordinating ligand set is denoted [OXO] (X = S[5], S$_2$[6], SO[7], P[8] for example), have now been reported.

Group 4 complexes incorporating [OXO] ligands have been identified as promising alkene polymerisation systems in the form {M[OXO]$_2$Cl$_2$}/MAO (MAO = methylalumoxane).[9] The bridging heteroatom, if coordinated, helps provide the stereochemically rigid framework essential for stereoregular polymer formation.[4] Density functional calculations show that a bridging sulfur atom increases the polymerisation rate by destabilising the π-bound intermediate [Ti(tbmp)Me-(H$_2$C=CH$_2$)]$^+$ {tbmp = 2,2′-thiobis(6-*tert*-butyl-4-methylphenol), an [OSO] ligand} with respect to the reactants.[10] Additionally, the calculations suggest that the unsaturated backbone provided by the phenolate plays an important role in stabilising the transition states. The titanium complexes [Ti(tbmp)X$_2$] (X = Cl, O*i*Pr) exhibit high catalytic activities for the polymerisation of ethene,[9] styrene[11] and dienes[12] when activated with MAO, and can also co-polymerise ethene and styrene.[13]

There are very few reports of the analogous zirconium(IV) complexes. The zirconium derivatives are reportedly far more air- and moisture-sensitive than their titanium counterparts and react less cleanly.[2] In contrast with zirconocene α-olefin polymerisation catalysts,[14] the Zr[OSO] complexes reported so far exhibit no catalytic activity.[2] We have recently introduced the use of the larger naphtholate analogues of [OSO] biphenolates, [1,1′-S(2-HOC$_{10}$H$_4$-*t*Bu$_2$-3,6)$_2$] (H$_2$**L**^{SN}), in order to stabilise the first sulfur-bridged bis(aryloxide) complexes of lanthanides;[15] the thionaphthol [**L**^{SN}] thus seemed better suited as a supporting ancillary ligand for zirconium(IV).

Herein, we report the first structurally characterised zirconium(IV) complexes supported by an [OSO] ligand set. Comparative investigations between H$_2$**L**^{SN} and tbmp have led us to synthesise and characterise a new family of Group 4 complexes of the general formula [M(**L**^{SN})X$_2$] (X = chloride, amide, alkyl; M = Ti, Zr). In addition, their stability and activity towards olefin polymerisation has been studied and compared with that of relevant tbmp analogues.

---

[a] School of Chemistry, The University of Nottingham,
University Park, Nottingham NG7 2RD, UK
Fax: (internat.) + 44-115-951-3563
E-mail: Polly.Arnold@Nottingham.ac.uk
[b] Institute of Inorganic Chemistry, Aachen University of Technology (RWTH),
Prof.-Pirlet-Strasse 1, 52074 Aachen, Germany

DOI: 10.1002/ejic.200400174

2 Results and Discussion

2.1 Halide Complexes Supported by L^{SN}

2.1.1 Reaction of K_2L^{SN} with $TiCl_4$·2THF

Treatment of the solvent-free dipotassium salt [$K_2\mathbf{L}^{SN}$] with [$TiCl_4$·2THF] in toluene results in the formation of the monomeric complex [Ti($\mathbf{L}^{SN}$)Cl_2·THF] (**1**), albeit in poor yield (18%). It is found that the bis(ligand) complex [Ti($\mathbf{L}^{SN}$)$_2$] (**2**) is consistently formed by over-reaction,[16] and is always initially present as one third of the product mixture irrespective of the reaction stoichiometry employed (Scheme 1).

The formation of the bis(ligand) complexes analogous to **2** in the reactions of chelating biphenols only becomes significant when the addition of ligand to metal is accelerated or conducted in the absence of a donating solvent.[16,17] Although single crystals of **2** were obtained from a diethyl ether solution at −30 °C, they were unsuitable for single-crystal X-ray diffraction analysis due to rapid loss of lattice solvent.

The ^{1}H NMR spectrum of **2** reveals the presence of two sets of aromatic signals for the ligand, indicating the presence of a single geometrical isomer out of the three possible ones. The *cis*-facial conformation of ligands in **2** (C_2), rather than a *trans*-facial (C_i) or *mer-trans* (D_{2d}) arrangement, affords two sets of ligand resonances. This has been observed previously in the bis[OOO]zirconium complex [Zr{(OC_6H_3*t*Bu-2-Me-4-CH_2-6)$_2$)O}$_2$] {[OOO] = 2-oxapropanediyl-1,3-bis(2-*tert*-butyl-4-methylphenol)},[17] and in the biphenolato bis[OCO]Zr complex {[OCO] = [2,2′-methylenebis(6-*tert*-butyl-4-methylphenol)}.[18] In **2**, this apparent C_2 symmetry is consistent with the coordination of both sulfur atoms. In contrast, the structurally characterised bis[ONO]titanium(IV) complex [Ti{($OC_6H_2Me_2$-2,4)$_2$NPr}$_2$] adopts the more familiar *trans-mer* conformation.[19]

High-temperature ^{1}H NMR spectroscopy of [D$_8$]toluene solutions of **2** do not show any processes that render the two aromatic rings of the ligands equivalent. Thus, besides the structural rigidity of **2** over an accessible temperature range, the thermal barrier to *fac-cis*/*fac-trans* isomerism is high.

2.1.2 Reaction of H_2L^{SN} with $TiCl_4$

The reaction of [$H_2\mathbf{L}^{SN}$] with neat $TiCl_4$ in hexane or toluene yields the THF-free complex **1a**, which is anticipated to be dimeric in solution[20] (Scheme 1). If triethylamine is added to precipitate the HCl by-product, only the bis(ligand) complex is isolated.[2] However, if THF is added, further conversion of **1** into **2** is slowed down but not eliminated completely, so that neither product is formed in good yield. Analytically pure **2** is most readily obtained in a synthetically useful yield of 70% by the protonolysis reaction of [$H_2\mathbf{L}^{SN}$] with [Ti(OEt)$_4$] (vide infra).

As an alternative route to **1**, a stoichiometric reaction of $H_2\mathbf{L}^{SN}$ with [Ti(NMe_2)$_2Cl_2$] was undertaken. Again, monitoring the reaction by ^{1}H NMR spectroscopy reveals the existence of a relatively short-lived species assigned as [Ti($\mathbf{L}^{SN}$)(Cl)NMe_2] (**3**) by comparison with related complexes, but its decomposition into **2** precludes further characterisation.

2.1.3 Preparation of 1 by Comproportionation

The synthesis of **1** is best achieved by comproportionation: Treatment of **2** with 1 equiv. of [$TiCl_4$·2THF] in a 4:1 mixture of dichloromethane/tetrahydrofuran at −60 °C (Scheme 1) affords, after warming to ambient temperature, a dark brown solution from which **1** may be isolated in 96% yield.

2.1.4 Reactions of [L^{SN}] with $ZrCl_4$·2THF

Treatment of stoichiometric solvent-free [$K_2\mathbf{L}^{SN}$] with [$ZrCl_4$·2THF] in toluene results in the formation of the colourless bis(ligand) complex [Zr($\mathbf{L}^{SN}$)$_2$·THF] (**5**) in an

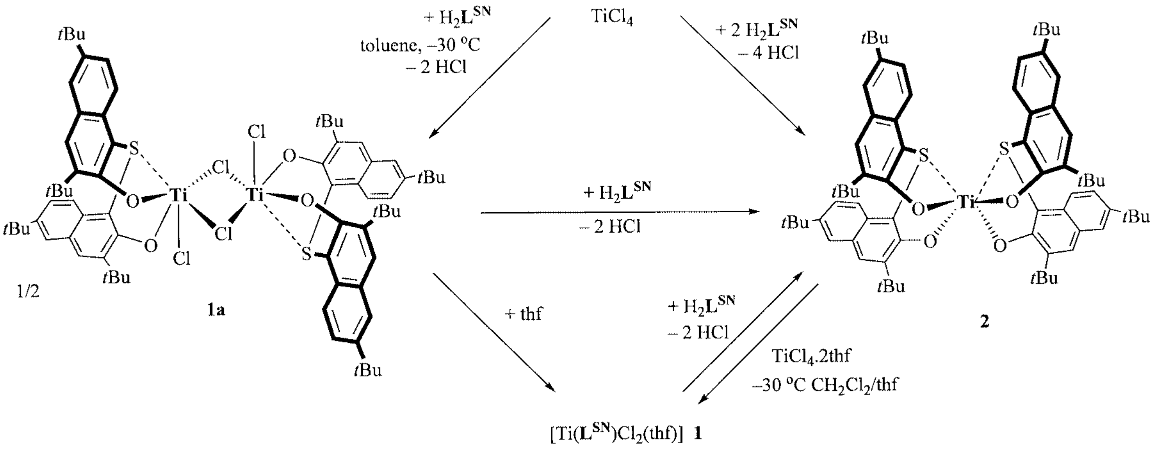

Scheme 1. Reactions of H_2L^{SN} with $TiCl_4$

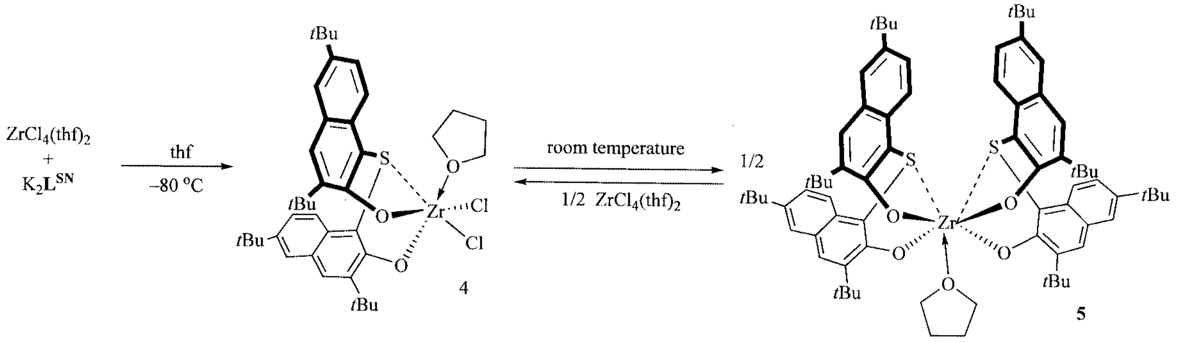

Scheme 2. Synthesis of $Zr^{IV}-L^{SN}$ adducts

isolated yield of 34% (Scheme 2). Single crystals of **5** suitable for X-ray diffraction were grown by slow cooling of a saturated diethyl ether solution of **5** to −30 °C. The comproportionation of **5** and [$ZrCl_4$·2THF] in THF affords the desired complex [Zr(L^{SN})Cl_2·THF] (**4**) in 53% yield.

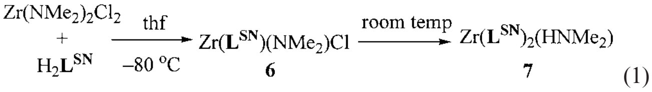

$$\underset{H_2L^{SN}}{\overset{Zr(NMe_2)_2Cl_2}{+}} \xrightarrow[-80\ ^{\circ}C]{thf} \underset{\mathbf{6}}{Zr(L^{SN})(NMe_2)Cl} \xrightarrow{room\ temp} \underset{\mathbf{7}}{Zr(L^{SN})_2(HNMe_2)} \qquad (1)$$

The protonolysis reaction of H_2L^{SN} with [$Zr(NMe_2)_2Cl_2$·2THF] yields the amido chloride **6** as an intermediate. Irrespective of the reaction solvent polarity, this rapidly undergoes a ligand redistribution reaction to form the amine-stabilised analogue of **5**, [$Zr(L^{SN})_2(HNMe_2)$] (**7**), as the major product [Equation (1)]. The coordinated molecule of $HNMe_2$ is retained in the product even when the reaction solvent is THF.

2.2 Single-Crystal X-ray Analysis of [$Zr(L^{SN})_2$·THF] (5)

Cooling of a concentrated diethyl ether solution of **5** to −30 °C affords single colourless blocks suitable for a X-ray diffraction study. The solid-state molecular structure (Figure 1) confirms the expected connectivity. Selected interatomic distances and angles are collected in Table 1.

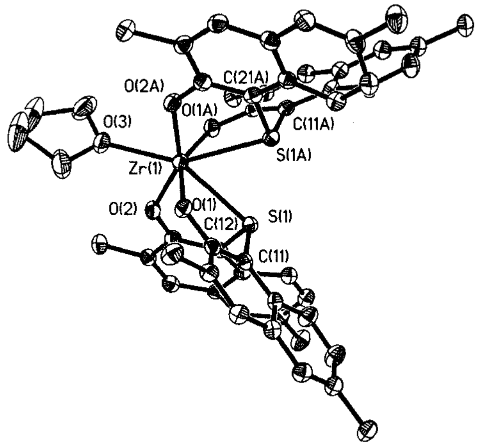

Figure 1. Thermal ellipsoid drawing of **5**·Et_2O (50% probability); methyl groups and solvent of crystallisation removed for clarity

The first significant feature of the molecular structure of **5** is the co-facial arrangement of the two binaphthol ligands, which imparts a distorted capped octahedral ge-

Table 1. Selected interatomic distances [Å] and angles [°] for **5**·Et_2O and **9** and **10**

5·Et_2O		**9**		**10**	
Zr(1)−O(1)	2.002(2)	Zr(1)−O(1)	1.981(2)	Zr(1)−O(1)	1.992(3)
Zr(1)−O(2)	2.087(2)	Zr(1)−O(2)	2.004(2)	Zr(1)−O(2)	1.986(3)
Zr(1)−O(3)	2.283(3)	Zr(1)−O(3)	2.259(2)	Zr(1)−O(5A)	2.136(3)
Zr(1)−S(1)	2.7657(8)	Zr(1)−S(1)	2.9248(7)	Zr(1)−S(1)	2.8881(13)
S(1)−C(21)	1.784(3)	Zr(1)−C(40)	2.296(3)	Zr(1)−O(5)	2.166(3)
S(1)−C(11)	1.799(3)	Zr(1)−C(50)	2.312(3)	Zr(1)−C(40)	2.228(5)
O(1)−C(12)	1.340(3)	Zr(1)−C(51)	2.850(3)	Zr(1)−Zr(1A)	3.4904(13)
O(2)−C(22)	1.331(3)	S(1)−C(21)	1.789(3)	S(1)−C(21)	1.790(5)
O(1)−Zr(1)−O(2)	93.71(8)	O(1)−Zr(1)−O(2)	92.94(8)	O(1)−Zr(1)−O(2)	95.10(14)
O(1)−Zr(1)−O(3)	104.94(6)	O(1)−Zr(1)−O(3)	166.14 (8)	O(2)−Zr(1)−O(5A)	91.63(14)
O(2)−Zr(1)−O(3)	75.59(5)	O(2)−Zr(1)−O(3)	83.54(8)	O(1)−Zr(1)−O(5A)	148.15(13)
O(1)−Zr(1)−S(1)	73.60(6)	O(1)−Zr(1)−C(40)	92.21(10)	O(2)−Zr(1)−C(40)	97.88(17)
O(2)−Zr(1)−S(1)	71.63(6)	O(2)−Zr(1)−C(40)	99.02(10)	O(2)−Zr(1)−S(1)	70.13(9)
O(3)−Zr(1)−S(1)	146.963(15)	O(1)−Zr(1)−C(50)	91.39(11)	O(1)−Zr(1)−S(1)	70.91(9)
O(2)−Zr(1)−S(1A)	137.09(6)	O(2)−Zr(1)−C(50)	140.56(10)	O(5A)−Zr(1)−S(1)	82.34(9)
O(3)−Zr(1)−S(1A)	146.963(15)	C(40)−Zr(1)−C(50)	119.96(12)	O(5)−Zr(1)−S(1)	91.14(9)
S(1)−Zr(1)−S(1A)	66.07(3)	O(1)−Zr(1)−S(1)	70.41(6)		
O(2A)−Zr(1)−S(1)	137.09(6)	O(2)−Zr(1)−S(1)	69.79(5)		
		O(3)−Zr(1)−S(1)	95.84(6)		

ometry on the seven-coordinate zirconium centre. The four naphtholate oxygen atoms describe the equatorial plane, while S(1) and S(1A) occupy approximate axial positions. The bound THF molecule resides in the apical site, opposite and in between the two sulfur atoms. However, the O(1)−Zr(1)−O(1A) and O(2)−Zr(1)−O(2A) angles are not linear, and are 150° and 94°, respectively. Naphtholate−zirconium bond lengths are in the range expected for zirconium−oxygen single bonds (observed range: 1.89−2.06 Å).[21] The C(11)−S(1)−C(21) bond angle of each thionaphthol ligand [109.6(1)°] is relatively large, and the naphthol wings are opened out slightly, enabling the sulfur atom to come into close proximity to the metal ion. As a result, a sulfur−zirconium interaction with a distance of 2.7657(8) Å is established.[22]

The C−S−C dihedral angle between the two naphthol planes of each ligand is 57°, and notably, the intramolecular S−S distance is 3.015 Å which is considerably shorter than the sum of the van der Waals radii of two S atoms (3.6 Å), and shorter than 3.33 Å (a single S−S bond plus 1.50 Å) − it was suggested that this value indicates a nonbonding interaction between two atoms (Figure 2).[23] This implies a significant intramolecular sulfur interaction in the solid state. The nonlinearity of the O(1)−Zr(1)−O(1A) and O(2)−Zr(1)−O(2A) moieties also suggests an S−S interaction that bends both *fac* ligands towards each other.

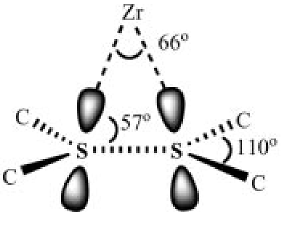

Figure 2. Suggested S−S (σ−π)-(π−π) interaction in **5** (for clarity, only the filled p orbital on each S atom is indicated); the dashed lines represent the Zr−S vector on the C_{2v} plane of each binaphthol ligand and the S−S interaction

Nonbonded intramolecular sulfur−sulfur interactions are relatively rare but can be energetically favourable. For example, the S_4 moiety in bis[8-(phenylthio)naphthyl] 1,1′-disulfide, which exhibits short nonbonded sulfur distances of 2.988(2) Å, is aligned in a linear fashion displaying two $n_p(S)$-σ*(S−S) 3-c-4-e bonds.[24] Nonbonding S interactions in this system are noted to have a greater influence on the solid-state geometry in the naphthalene complexes than in the corresponding phenyl disulfide. In the same way, the p-type lone pair orbital of Se in the R−Se−R′ fragments (R ≠ R′ = alkyl/aryl) has also been shown to play an important role in intramolecular nonbonding interactions.[25]

Ab initio calculations and statistical studies indicate that S···S close contacts in R−S−R fragments (R = H, alkyl, aryl) are attractive for a range of orientations (i.e. for a range of dihedral angles between the C_{2v} axis of each fragment), and there is a maximum probability for a colinear S···S arrangement.[26] Although calculations show that at short distances (3 Å) the interactions are mainly repulsive,[27,28] the dispersion contribution, which is substantial for the large, polarisable sulfur atom, provides an important attractive force that is able to compensate the repulsive electrostatic force. In **5**, the hard metal ion binds a molecule of THF, and the sulfur−sulfur dipole interaction is preferred over the formation of closer dative bonds between the metal and the soft sulfur atoms.

2.3 Alkyl Derivatives of L^{SN}

2.3.1 Dialkyltitanium Complexes

Attempts to prepare the dibenzyl complex $[Ti(\mathbf{L^{SN}})(CH_2Ph)_2]$ by protonolysis of $[Ti(CH_2Ph)_4]$ with $[H_2\mathbf{L^{SN}}]$ resulted only in the recovery of starting materials. This contrasts with the facile preparation of the biphenolate complex $[(tbmp)Ti(CH_2Ph)_2]$.[2] ^1H NMR spectroscopy suggests the formation of $[Ti(\mathbf{L^{SN}})(CH_2Ph)_2]$ (**8**) by metathesis between **1** and the Grignard reagent $PhCH_2MgCl$, but no tractable product could be isolated.

In an attempt to synthesise a dimethyl complex $[Ti(\mathbf{L^{SN}})Me_2]$, a hexane solution of **1** was treated with 2 equiv. of LiMe.[29] However, even at temperatures below −10 °C, the reaction mixture quickly became dark to yield an intractable mixture of products. A one-pot reaction at −80 °C of $H_2\mathbf{L^{SN}}$ with 4 equiv. of LiMe, followed by addition of $TiCl_4$, also yielded no tractable product.

2.3.2 Dibenzylzirconium Complexes

In contrast to the tetrabenzyltitanium reaction, treatment of 1 equiv. of $[H_2\mathbf{L^{SN}}]$ with tetrabenzylzirconium in THF results in the rapid formation of the bis(ligand) THF adduct **5**. No intermediates were detectable (by solution NMR spectroscopy) during the course of this reaction. This route to **5** gives higher yields than metathesis reactions with zirconium tetrachloride.

$$ZrBz_4 + H_2\mathbf{L^{SN}} \xrightarrow[-80\ ^{\circ}C]{thf} \underset{\mathbf{9}}{Zr(\mathbf{L^{SN}})(CH_2Ph)_2(thf)} \qquad (2)$$

A synthetic scale-up of the reaction (about 2.0 g) sufficiently reduces the extent of ligand redistribution to permit the isolation of the dibenzyl complex **9** as a pale yellow solid in moderate yield (47%) [Equation (2)]. This complex is significantly less sensitive to light than the parent alkyl compound, and if the reaction is carried out in the absence of donating solvents, an intractable product mixture results. The ^1H NMR spectroscopic resonances ($[D_6]$benzene) for the methylene benzyl moieties appear as a singlet at δ = 2.67 ppm, rather than an AB quadruplet.[30] Low-temperature ^1H NMR studies in $[D_8]$toluene and CD_2Cl_2 reveal no fluxional process slower than the NMR timescale that would render the two methylene protons inequivalent.[31]

2.3.3 Single-Crystal X-ray Analysis of $[Zr(L^{SN})(CH_2Ph)_2{\cdot}THF]$ (9)

The molecular structure of **9** is shown in Figure 3. It is evident that the metal atom maintains a mononuclear environment, and the bound THF molecule occupies an apical coordination site of a distorted octahedron. The ligand facially caps the zirconium atom, with relatively short naphtholate oxygen−zirconium distances of 1.981(2) and 2.004(2) Å for O(1) and O(2), respectively. The sulfur atom is geometrically placed in a *trans* arrangement to C(40) of the η^1-benzyl group, with a correspondingly long sulfur−zirconium distance of 2.9248(7) Å. As a result, the mean planes of the two naphthalene rings of the ligands form a dihedral angle of 78.0°, with an associated C(11)−S(1)−C(21) bond angle of 106.3(1)°.

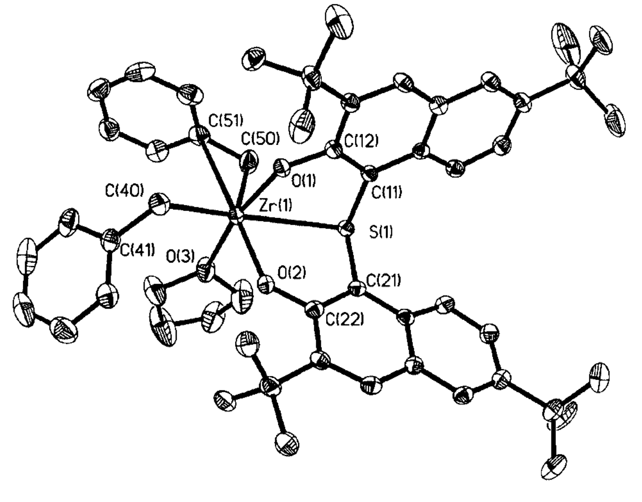

Figure 3. Molecular structure of **9**; view along the 100 plane; ellipsoids set at the 50% probability level; H atoms removed for clarity

The two coordinated benzyl groups are clearly distinguishable in the solid state, and display η^1- and η^2-bonding modes.[30] The η^2-bound benzyl ring [C(50), (C51)] has an acute Zr(1)−C(50)−C(51) angle of 95.3(2)°, in contrast to that of the η^1-benzyl group [Zr(1)−C(40)−C(41) 118.8(2)°]. The acuteness of this angle results in the close proximity of the phenyl ring to the zirconium atom, and in particular gives rise to a short Zr−C_{ipso} interaction of 2.850(3) Å.[30]

2.3.4 Reactivity of 9 with Air

Exposure of dibenzyl compound **9** to air affords three compounds, which can be identified by ^{1}H NMR spectroscopy [Equation (3)]. To date, we have been unable to isolate the analytically pure major product by recrystallisation, but were able to obtain single crystals suitable for structure analysis to confirm the identity. The complex is formally the product of the insertion of one oxygen atom per metal atom into the Zr−C bond of a benzyl group. The controlled O atom insertion into a bound alkyl group at an early transition metal is unusual,[32] and to the best of our knowledge, this is the first time a benzyl group has been selectively oxygenated. Usually, reaction with an oxygen atom source such as pyridine *N*-oxide or trimethylamine *N*-oxide, or air or water, forms oxo adducts containing the Zr−O−Zr unit.[33] Treatment of the dibenzyl complex **9** with trimethylamine *N*-oxide shows that the same product is formed, confirming that **10** derives from the reaction with air; but while the yield is greatly improved for this reaction, we were unable to obtain correct elemental analysis data for this complex. Work is in progress to identify whether the oxidisable sulfur bridge is involved in this oxygen atom insertion into the Zr−C bond.

9

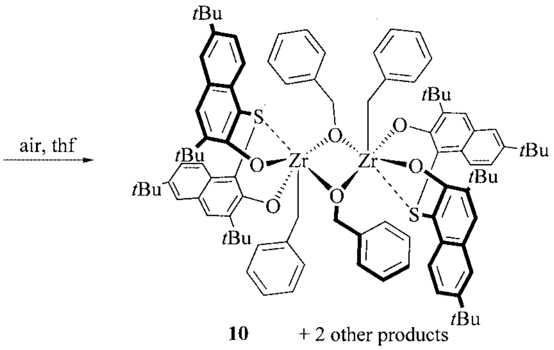

10 + 2 other products

(3)

The molecular structure of **10** (Figure 4) is dinuclear and unsolvated. The geometry at Zr is essentially octahedral with a *fac*-$\mathbf{L}^{SN}$ ligand, a small cone angle of the [OSO] group and a relatively long Zr(1)−S(1) contact of 2.8881(13) Å. The remaining benzyl group shows no additional agostic interaction with the metal atom. The oxygenated benzyl group bridges the zirconium centre and its symmetry-related equivalent in a nearly symmetrical fashion with an average Zr−O distance of 2.15 Å, relative to an average Zr−$O_{naphtholate}$ distance of 1.99 Å, and a Zr−Zr′ distance of 3.490(1) Å.

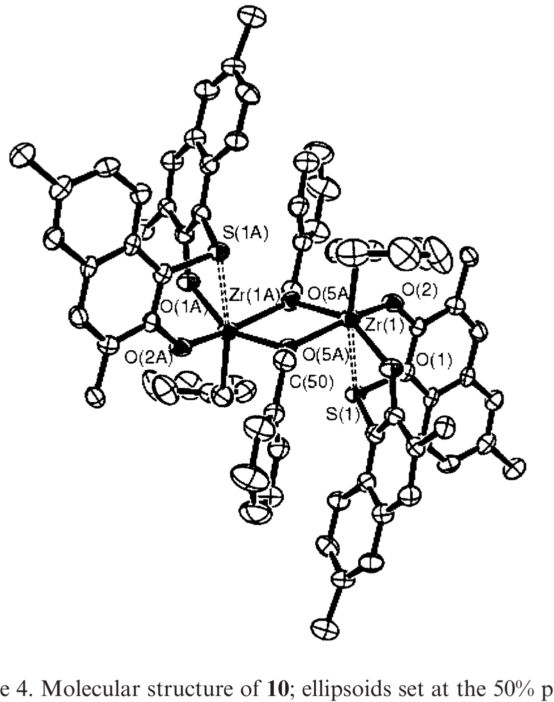

Figure 4. Molecular structure of **10**; ellipsoids set at the 50% probability level; solvent and Me groups removed for clarity

Interestingly, the Zr−S distances in both [Zr($\mathbf{L}^{SN}$)$_1$X$_2$] complexes are longer than those in the sterically more congested [Zr($\mathbf{L}^{SN}$)$_2$] complex, giving further weight to the at-

Table 2. Results for the polymerisation of ethene and propene

Complex (mmol)	Yield [g]	Time [min]	Activity[a]	M_w[b] (× 10^5)	M_n [b]	M_w/M_n [b]
1 [Ti(**L**^{SN})Cl_2·THF] (0.027)[c]	7.92	60	29	2.04	46900	4.4
4 [Zr(**L**^{SN})Cl_2·THF] (0.026)[c]	0.26	60	1	8.36	28000	30
9 [Zr(**L**^{SN})$(CH_2Ph)_2$·THF] (0.023)[c]	5.95	60	26	0.22	4300	5.25
[(tbmp)$TiCl_2$] (0.02)[d]	7.90	5	1580	3.5	29000	11.9
[(tbmp)$TiCl_2$]$_2$ (0.0025)[e]	0.55	60	220	0.12	8000	2.2
[(tbmp)$ZrCl_2$] (0.02)[f]	inactive					
1 (0.027)[g]	4.22	60	15	0.02	510	4.1

[a] Activities quoted in kg PE mol^{-1}[catalyst] bar^{-1} h^{-1}. [b] PDI determined by GPC, results are an average of two runs. [c] Conditions used: 20 °C, 20 mg of catalyst, 1000 equiv. of MAO in 150 mL of toluene, 10 bar of ethene/propene, 1 h. [d] Results taken from ref.[2], run at 40 °C, 3 bar of ethene, 500 equiv. of MAO in 200 mL of toluene. [e] Result taken from ref.[20], run at 20 °C, 1 bar of ethene, 1000 equiv. of MAO in toluene. [f] Results taken from ref.[2], run at 20 °C, 3 bar of ethene, 500 equiv. of MAO in 200 mL of toluene. [g] 10 bar of propene.

tractive S−S interaction's dominance of the local geometry of the ligands in the bis(ligand) complex **5**.

2.4 Polymerisation of Ethene and Propene

Three suitable complexes were chosen for the polymerisation studies, [Ti(**L**^{SN})Cl_2·THF] (**1**), [Zr(**L**^{SN})Cl_2·THF] (**4**) and [Zr(**L**^{SN})$(CH_2Ph)_2$·THF] (**9**). The results are collated in Table 2; for comparison, the analogous tbmp complexes have been included. A significant exotherm was observed during the first 10 min of each polymerisation run (except **4**/MAO), attaining a maximum temperature of 50 °C. For the remainder of each polymerisation run, the autoclave temperatures remained almost constant (within 5 °C).

The titanium dichloride system **1**/MAO and the bis(benzyl)zirconium complex **9**/MAO exhibit moderate activities for the polymerisation of ethene and produce polyethene with high molecular weights, whereas the corresponding zirconium chloride system **4**/MAO shows a much lower propensity to polymerise ethene. Under identical conditions, **1**/MAO also shows moderate activity for the polymerisation of propene. Theory suggests that the Ti-based catalysts are more active than their zirconium counterparts due to a slightly lower activation energy barrier;[10] the complete inactivity of the (tmbp)Zr species is therefore surprising.

The ethene polymerisation activity of **1**/MAO (28.94 kg PE mol^{-1}[Ti] bar^{-1} h^{-1}) compares well with the dimeric complex [(tbmp)$TiCl_2$]$_2$, which was tested at a lower catalyst concentration (220 kg PE mol[Ti]$^{-1}$ bar^{-1} h^{-1}).[20] However, the binaphthol-based catalyst remains an order of magnitude less active than the corresponding biphenol system. Theoretical studies also suggested that the catalyst activity is influenced by the extent of conjugation in the ligand backbone and that a C=C bridged system should be more active than a C−C system.[2,10] The naphthol bridge in these systems, which has a lower aromaticity than a phenol, supports this argument.

However, the Zr naphtholate systems are better catalysts than their phenolate counterparts. In view of the inactivity of the reported Zr-based biphenolates towards ethene polymerisation, these results are encouraging. Narrow molecular weight distributions and polydispersities for the sample isolated from the **1**/MAO/ethene run suggest that this a well-defined single-site catalyst. This is in contrast to the higher PDI reported for the [(tbmp)$TiCl_2$]/MAO system run for a brief period of time.[2] The polyolefin from the **1**/MAO/propene run was isolated as a viscous oil, with a low average molecular weight for the polymer. The molecular weight distribution appears bimodal, suggesting an ill-defined active catalyst species and/or the presence of more than one active site. Again, a bimodal distribution is apparent in the **4**/MAO/ethene system.

2.5 Conclusions

Titanium(IV) and zirconium(IV) complexes supported by the binaphtholate **L**^{SN} dianion have been synthesised and structurally characterised. The formation of bis(**L**^{SN}) complexes renders the direct syntheses of titanium(IV) and zirconium(IV) dichloride complexes difficult, with possible further stabilisation of the zbis(**L**^{SN})irconium complex by an S−S interaction. However, unlike aminebis(phenolate) [ONO] derivatives of Group 4 metals, the bis[OSO] complexes undergo disproportionation reactions to form heteroleptic adducts.

The first crystallographically characterised Zr[OSO] complexes have been isolated. The bis(OSO)zirconium THF adduct exhibits a co-facial arrangement of the naphthol ligands, a distorted capped octahedral geometry at Zr and close S−S distances, which suggest an unusual noncovalent S···S interaction in the solid state. The zirconium [OSO] complexes are kinetically more labile than related aminebis(phenolate) [ONO] adducts, but less labile than their titanium counterparts, and heteroleptic complexes are easier to isolate. The dibenzylzirconium complex reacts with air to insert an O atom rather than decompose to a μ-oxodizirconium complex. Preliminary reactions with the oxygen atom source trimethylamine *N*-oxide show that the same product is formed. Structural studies of the complexes have shown that the smaller Group 4 metal cations accommodate the symmetrical *fac* conformation of the **L**^{SN} ligand much more readily than the twisted conformation observed in the corresponding lanthanide chemistry.[15,34]

The complexes **1** and **9** are effective ethene polymerisation pre-catalysts, whereas the dichloride **4** displays a surprisingly low activity towards ethene polymerisation. The catalyst system **1**/MAO is also moderately active for the polymerisation of propene.

3. Experimental Section

General Procedures: All experimental procedures were performed under dry, oxygen-free argon or dinitrogen, with standard Schlenk techniques (mechanical pump for vacuum 10^{-4} mbar). Subsequent manipulations of isolated compounds were carried out in a glove box (MBraun Unilab) under dry dinitrogen. All ^{1}H and ^{13}C NMR spectra were recorded with a Bruker DPX 300 spectrometer, operating frequency variable temperature unit at 300 K, unless otherwise stated. Chemical shifts are reported in parts per million and referenced to residual proton resonances in [D$_6$]benzene calibrated against external TMS. Mass spectra (EI and FAB) were run by Dr. Ali Abdul-Sada with a Kratos MS80RF instrument. Elemental analyses were determined by Dr. Stephen Boyer at London Metropolitan University and by Mr. Trevor Spencer at the University of Nottingham. Polymerisation runs were conducted in a purpose-built rig in the laboratory of Professor F. G. N. Cloke, at the University of Sussex, and GPC analysis was performed by Rapra Technology Ltd. A glass autoclave with a magnetically coupled stirrer was charged with a toluene solution of each complex, 1000 equiv. of MAO, and the vessel pressurised at 20 °C with 10 bar of ethene or 10 bar of propene for 1 h. Samples from the **1**/MAO/ethene and **4**/MAO/ethene were found to contain a significant amount of insoluble (in 1,2,3-trichlorobenzene) material and were difficult to filter. The chromatogram peak area for **4**/MAO/ethene is less than 20% that of the **1**/MAO/ethene and **9**/MAO/ethene samples, suggesting that the bulk of this sample remained insoluble. The insolubility of the polymer could be due to an exceptionally high molecular weight or a high degree of cross-linking. All solvents used (toluene, THF, diethyl ether, hexane, dichloromethane) were either degassed and purified by passage through activated alumina towers prior to use, or were freshly distilled from the appropriate alkali metal under dinitrogen, and thoroughly degassed prior to use. NMR spectroscopic grade [D$_6$]benzene and [D$_8$]toluene were refluxed over potassium metal, and CD_2Cl_2 refluxed over CaH_2 and vacuum-distilled before use. All chemicals were either obtained from Aldrich Chemicals, except *n*BuLi and sulfur dichloride (Acros), or were synthesised according to standard literature procedures.[35] Literature procedures for the preparation of [1,1′-S(2-HOC$_{10}$H$_4$*t*Bu$_2$-3,6)$_2$] (H$_2$**L**^{SN})[15] and [1,1′-S(2-KOC$_{10}$H$_4$*t*Bu$_2$-3,6)$_2$(THF)$_2$] (K$_2$**L**^{SN})[36] have previously been described.

[(L^{SN})TiCl$_2$·THF] (1): A solution of TiCl$_4$·2THF in THF (30 mg, 0.09 mmol, 10 mL) was added dropwise to a solution of **2** in a 1:1 mixture of THF/dichloromethane (0.1 g, 0.09 mmol, 30 mL) cooled to −78 °C. The reaction mixture was left to warm slowly to ambient temperature, upon which it changed colour from orange to dark brown. After 12 h, all volatiles were removed under reduced pressure. The crude product was extracted into hexane and cooled to −30 °C. Analytically pure **1** was isolated as a microcrystalline brown solid in 96% yield (62 mg). ^{1}H NMR (C$_6$D$_6$): δ = 8.66 (d, $^3J_{H,H}$ = 8.85 Hz, 1 H, 8-H), 7.51 (s, 3H 4-H, 5-H, 7-H), 3.81 (br., 2 H, CH$_2$ THF), 1.62 (s, 9 H, 3-*t*Bu), 1.32 (br., 2 H, CH$_2$ THF), 1.19 (s, 9 H, 6-*t*Bu) ppm. $C_{36}H_{44}Cl_2O_2STi·THF$ (731.71): calcd. C 65.66, H 7.16; found C 65.67, H 7.39.

[(L^{SN})Ti(μ-Cl)Cl]$_2$ (1a): ^{1}H NMR/C$_6$D$_6$: δ = 8.61 (br., 1 H, 8-H), 7.38 (m, 3H 4-H, 5-H, 7-H), 1.48 (s, 9 H, 3-*t*Bu), 1.18 (s, 9 H, 6-*t*Bu) ppm.

[(L^{SN})$_2$Ti] (2): A solution of **H$_2$L^{SN}** in THF (0.2 g, 0.37 mmol, 15 mL) was added dropwise to a cooled solution of Ti(OEt)$_4$ in THF (19.0 μL, 0.185 mmol, 10 mL) at −30 °C over a period of 20 min, and the mixture was warmed to room temperature over 12 h, by which time **2** had precipitated from the reaction mixture. The supernatant was decanted from the precipitate, and the crude powder washed with 3 × 10 mL cold hexane to yield analytically pure **2** in 70% yield (0.146 g). ^{1}H NMR (C$_6$D$_6$): δ = 8.93 (br., 1 H, 8-H), 8.87 (br., 1 H, 8-H), 7.59 (m, 6 H, 4-H, 5-H, 7-H), 1.67 (s, 9 H, 3-*t*Bu), 1.59 (s, 9 H, 3-*t*Bu), 1.23 (s, 9 H, 6-*t*Bu) ppm. EI-MS: *m*/*z* (%)= 1128 (24) [M$^+$]. $C_{72}H_{88}O_4S_2Ti$ (1128): calcd. C 76.56, H 7.85; found C 76.48, H 7.80.

[(L^{SN})Ti(μ-NMe$_2$)Cl]$_2$ (3a): ^{1}H NMR (C$_6$D$_6$): δ = 8.48 (d, $^3J_{H,H}$ = 8.82 Hz, 1 H, 8-H), 7.58 (m, 3H 4-H, 5-H, 7-H), 1.78 (s, 3 H, NMe$_2$), 1.16 (s, 9 H, 3-*t*Bu), 1.31 (s, 9 H, 6-*t*Bu) ppm.

[(L^{SN})Ti(μ-Cl)NMe$_2$]$_2$ (3b): ^{1}H NMR: δ = 8.79 (d, $^3J_{H,H}$ = 8.70 Hz, 1 H, 8-H), 7.58 (m, 3H 4-H, 5-H, 7-H), 1.78 (s, 3 H, NMe$_2$), 1.26 (s, 9 H, 3-*t*Bu), 1.71 (s, 9 H, 6-*t*Bu) ppm.

[(L^{SN})ZrCl$_2$·THF] (4): A slurry of ZrCl$_4$·2THF in toluene (21 mg, 0.056 mmol, 7 mL) was added dropwise over a period of 20 min to a solution of **5** in toluene (70 mg, 0.056 mmol, 7 mL),which was cooled to −60 °C. The resultant solution was allowed to slowly attain room temperature over 4 h and stirred at room temperature for a further 10 h. All volatiles were removed under reduced pressure, and the crude product extracted into hexane (15 mL). Cooling to −30 °C afforded a colourless precipitate that was isolated and washed with cold hexane (3 × 5 mL) to give analytically pure **4** in 53% yield (0.021 g). ^{1}H NMR (C$_6$D$_6$): δ = 8.83 (br., 1 H, 8-H), 7.58 (m, 3 H, 4-H, 5-H, 7-H), 3.70 (br., 4 H,CH$_2$ THF), 1.58 (br., 9 H,3-*t*Bu), 1.35 (br., 4 H, CH$_2$ THF), 1.23 (s, 9 H, 6-*t*Bu) ppm. $C_{36}H_{44}Cl_2O_2SZr·THF$ (775.1): calcd. C 61.98, H 6.76; found C 61.47, H 7.03.

[(L^{SN})$_2$Zr·THF] (5): In the absence of light, a solution of H$_2$L^{SN} in THF (500 mg, 0.92 mmol, 20 mL) was added dropwise to a solution of Zr(CH$_2$Ph)$_4$ in THF (210 mg, 0.46 mmol, 15 mL), which was cooled to −60 °C over 30 min. Upon completion of the addition of the ligand, the reaction mixture was slowly warmed to room temperature and stirred at ambient temperature for a further 10 h. All volatiles were removed under reduced pressure, and the crude solid extracted into 5 mL of diethyl ether. Subsequent cooling to −30 °C afforded single crystals suitable for X-ray diffraction analysis in 45% yield (258 mg). ^{1}H NMR (C$_6$D$_6$): δ = 8.80 (d, $^3J_{H,H}$ = 8.97 Hz, 1 H, 8-H), 7.64 (s, 1 H, 4-H), 7.57 (s, 1 H, 5-H), 7.11 (d, $^3J_{H,H}$ = 8.97 Hz, 1 H, 7-H), 4.10 (br., 2 H, CH$_2$ THF), 1.57 (s, 9 H, 3-*t*Bu), 1.36 (br., 2 H, CH$_2$ THF) 1.23 (s, 9 H, 6-*t*Bu) ppm. $C_{72}H_{88}O_4S_2Zr·THF$ (1245.0): calcd. C 73.37, H 7.77; found C 73.19, H 7.54.

[(L^{SN})Zr(μ-NMe$_2$)Cl]$_2$ (6a): ^{1}H NMR (C$_6$D$_6$): δ = 8.81 (br., 2 H, 8-H), 7.56 (m, 6 H, 4-H, 5-H, 7-H), 3.85 (s, 3 H, μ-NMe$_2$), 1.66 (s, 18 H, 3-*t*Bu), 1.23 (s, 18 H, 6-*t*Bu) ppm.

[(L^{SN})Zr(μ-Cl)NMe$_2$]$_2$ (6b): ^{1}H NMR (C$_6$D$_6$): δ = 8.76 (d, $^3J_{H,H}$ = 8.76 Hz, 2 H, 8-H), 7.56 (m, 6 H, 4-H, 5-H, 7-H), 1.61 (s, 3 H, NMe$_2$), 1.58 (s, 18 H, 3-*t*Bu), 1.19 (s, 18 H, 6-*t*Bu) ppm.

[(L^{SN})$_2$Zr·HNMe$_2$] (7): ^{1}H NMR (C$_6$D$_6$): δ = 8.67 (br., 2 H, 8-H,), 7.59 (s, 2 H, 4-H), 7.55 (br., 2 H, 7 H), 7.44 (d, $^3J_{H,H}$ = 8.74 Hz, 2 H, 7-H), 2.66 (br., 3 H, $HNMe_2$) 1.53 (s, 18 H, 3-*t*Bu), 1.23 (s, 18 H, 6-*t*Bu) ppm.

[(L^{SN})Ti(CH_2Ph)$_2$] (8): ^{1}H NMR (C_6D_6): δ_H = 8.69 (d, $^3J_{H,H}$ = 9.03 Hz, 1 H, 8-H), 7.51 (m, 3H 4-H, 5-H, 7-H), 7.05 (m, 5 H, CH_2*Ph*) 2.10 (s, 2 H, C*H*$_2$Ph), 1.62 (s, 9 H, 3-*t*Bu), 1.17 (s, 9 H, 6-*t*Bu) ppm.

[(L^{SN})Zr(CH_2Ph)$_2$·thf] (9): A solution of H_2L^{SN} in THF (2.0 g, 3.69 mmol, 25 mL) was added dropwise to a solution of $Zr(CH_2Ph)_4$ in THF (1.68 g, 3.69 mmol, 15 mL), which was cooled to −60 °C over 45 min. Upon completion of addition of the ligand, the reaction mixture was slowly warmed to room temperature and stirred for a further 15 h. All volatiles were removed under reduced pressure, and the crude solid extracted into 25 mL of diethyl ether. Cooling of the solution to −30 °C resulted in the precipitation of analytically pure **10** as a yellow powder, which was washed with 3 × 5 mL cold diethyl ether, and isolated in 47% yield (1.54 g). Single crystals suitable for X-ray diffraction studies were grown from slow concentration of the supernatant at −30 °C. ^{1}H NMR (C_6D_6): δ = 8.94 (d, $^3J_{H,H}$ = 8.76 Hz, 1 H, 8-H), 7.62 (s, 1 H, 4-H), 7.60 (s, 1 H, 7-H), 7.57 (s, 1 H, 5-H), 7.55 (m, 2 H, CH_2Ph), 6.87 (m, 3 H, CH_2Ph), 3.53 (br., 2 H, CH_2 THF), 2.67 (s, 2 H, CH_2Ph), 1.56 (s, 9 H, 3-*t*Bu), 1.24 (s, 9 H, 6-*t*Bu), 1.01 (br., 2 H, CH_2 THF) ppm. ^{13}C NMR (C_6D_6): δ = 166.68, 130.00, 129.67, 129.28 (quaternary C), 145.49, 140.10, 137.85, 133.39, 127.68, 126.17, 125.65 (CH), 65.48 (CH_2Ph) 31.34, 30.08 (*t*Bu), 73.18, 25.05 (THF) ppm. $C_{50}H_{54}O_2SZr$·thf (882.4): calcd. C 73.22, H 7.46; found C 73.49, H 7.69.

[(L^{SN})Zr(OCH_2Ph)(CH_2Ph)$_2$] (10). a) A Schlenk tube containing powdered **9** was exposed to air for 2 min. The resulting colourless powder was recrystallised from diethyl ether, from which crystals of **10** suitable for single-crystal X-ray diffraction were isolated. **b)** Under N_2, a glass vial was charged with a [D$_6$]benzene solution of **9** (20 mg, 22.6 μmol), and a [D$_6$]benzene solution of Me_3NO (1.6 mg, 22.6 μmol). The resultant mixture was filtered through glass wool into a Young's PTFE tap equipped NMR tube, and a ^{1}H NMR spectrum recorded immediately. The reaction was further monitored by ^{1}H NMR spectroscopy. *t* = 0 h: The ^{1}H NMR spectroscopic resonances of **9** have completely given way to a new transient species (not identified) and **10** in a 1:1 ratio. ^{1}H NMR (C_6D_6) of **10**: δ = 8.98 (d, $^3J_{H,H}$ = 8.46 Hz, 1 H, 8-H), 7.61 (m, 9 H, Ar), 3.59 (br., 1 H, OC*H*$_2$), 3.25 (br., 1 H, C*H*$_2$), 1.73 (s, 9 H, 3-*t*Bu), 1.26 (s, 9 H, 6-*t*Bu) ppm. $C_{50}H_{58}O_3SZr$ (830.3): calcd. C 72.32, H 7.04; found C 67.01, H 7.96. Yield, isolated from a mixture with **9** (42 mg, 1.4%). ^{1}H NMR (C_6D_6) of transient: δ = 9.16 (d, $^3J_{H,H}$ = 8.94 Hz, 1 H, 8-H), 7.41 (m, 9 H, Ar), 2.94 (br., 1 H, C*H*$_2$), 1.68 (s, 9 H, 3-*t*Bu), 1.45 (s, 9 H, 6-*t*Bu) ppm. *t* = 1 h: The ^{1}H NMR spectroscopic resonances due to **10** have grown considerably, while those for the transient species have decreased to a ratio of 5:2. *t* = 24 h: ^{1}H NMR spectrum contains a few more resonances of insignificant integral value but is essentially unchanged. *t* = 168 h: No change in ^{1}H NMR spectrum.

Crystallographic Data: X-ray data (Table 3) were collected using Mo-K_α radiation (λ = 0.71073 Å) with a Bruker SMART1000 CCD area detector diffractometer using ω scans. Structure solution and refinement was carried out with the SHELX suite of programs.[37] CCDC-217721 (**5**), -217722 (**9**) and -217723 (**10**) contain the supplementary crystallographic data for this paper. These data can be obtained free of charge at www.ccdc.cam.ac.uk/conts/retrieving.html [or from the Cambridge Crystallographic Data Centre, 12 Union Road, Cambridge CB2 1EZ, UK; Fax: (internat.) + 44-1223-336-033; E-mail: deposit@ccdc.cam.ac.uk].

Table 3. Crystallographic data and structure refinement for **5**·Et_2O and **9** and **10**

Empirical formula	$C_{80}H_{106}O_6S_2Zr$ (**5**·Et_2O)	$C_{54}H_{66}O_3SZr$ (**9**)	$C_{54}H_{68}O_4SZr$ (**10**)
Formula mass	1319.07	886.35	1808.73
Temperature [K]	150(2)	293(2)	150(2)
Wavelength [Å]	0.71073	0.71073	0.71073
Crystal system	monoclinic	monoclinic	monoclinic
Space group	*C*2/*c*	*P*2$_1$/*n*	*P*2$_1$/*n*
Unit cell dimensions	*a* = 33.175(2) Å	*a* = 16.5541(11) Å	*a* = 14.815(3) Å
	b = 11.2138(8) Å	*b* = 11.1071(8) Å	*b* = 21.612(4) Å
	c = 21.746(2) Å	*c* = 25.9090(18) Å	*c* = 16.183(3) Å
	β = 105.1690(10)°	*β* = 91.2190(10)°	β = 108.630(4)°
Volume [Å^3]	7808.0(10)	4762.8(6)	4910.1(15)
Z	4	4	2
$D_{calcd.}$ [Mg/m^3]	1.137	1.236	1.223
Absorption coefficient [mm^{-1}]	0.242	0.316	0.309
F(000)	2856	1880	1920
Crystal size [mm]	0.27 × 0.20 × 0.12	0.4 × 0.15 × 0.10	0.22 × 0.20 × 0.14
θ range for data collection [°]	1.92−26.37	2.21−29.04	1.73−28.77
Index ranges	$-42 \le h \le 44$	$-22 \le h \le 22$	$-18 \le h \le 9$
	$-14 \le k \le 14$	$-13 \le k \le 15$	$-26 \le k \le 27$
	$-28 \le l \le 29$	$-34 \le l \le 35$	$-7 \le l \le 21$
Reflections collected	35011	31092	16297
Independent reflections	7969 [*R*(int) = 0.049]	11709 [*R*(int) = 0.053]	8782 [*R*(int) = 0.0691]
Completeness to θ = 26.37°	99.8%	99.2%	76.2%
Absorption correction	Semi-empirical from equivalents	Semi-empirical from equivalents	None
Max. and min. transmission	0.904 and 0.864	1.000 and 0.870	
Refinement method	Full-matrix least squares on F^2	Full-matrix least squares on F^2	Full-matrix least squares on F^2
Data/restraints/parameters	7969/38/419	11709/0/532	8782/0/486
Goodness-of-fit on F^2	1.016	1.054	0.895
Final *R* int [$I > 2\sigma(I)$]	*R*1 = 0.0476, *wR*2 = 0.1293	*R*1 = 0.0581, *wR*2 = 0.1142	*R*1 = 0.0570, *wR*2 = 0.1302

Acknowledgments

The authors thank the EPSRC (studentship for L. S. N., Advanced Fellowship for P. L. A.) and the Royal Society for funding, Professor F. Geoffrey N. Cloke for use of a catalyst testing apparatus, and the Deutsche Forschungsgemeinschaft and the Fonds der Chemischen Industrie for financial support.

---

[1] V. C. Gibson, S. K. Spitzmesser, *Chem. Rev.* **2003**, *103*, 283.

[2] A. Van der Linden, C. J. Schavarien, N. Meijboom, C. Ganter, G. Orpen, *J. Am. Chem. Soc.* **1995**, *117*, 3008.

[3] V. C. Gibson, *J. Chem. Soc., Dalton Trans.* **1994**, 1607.

[4] G. J. P. Britosvek, V. C. Gibson, D. F. Wass, *Angew. Chem. Int. Ed.* **1999**, *38*, 428.

[5] S. Fokken, T. P. Spaniol, H.-C. Kang, W. Massa, J. Okuda, *Organometallics* **1999**, *15*, 5069; L. Porri, A. Ripa, P. Colombo, E. Miano, S. Capelli, S. V. Meille, *J. Organomet. Chem.* **1996**, *514*, 213; F. Amor, S. Fokken, T. Kleinheim, T. P. Spaniol, J. Okuda, *J. Organomet. Chem.* **2001**, *621*, 3; Y. Takashima, Y. Nakayama, H. Yasuda, A. Nakamura, A. Harada, *J. Organomet. Chem.* **2002**, *654*, 74.

[6] J. Okuda, S. Fokken, T. Kleinhenn, T. P. Spaniol, *Eur. J. Inorg. Chem.* **2000**, 1321; C. Capacchione, A. Proto, H. Ebeling, R. Muelhaupt, K. Moeller, T. P. Spaniol, J. Okuda, *J. Am. Chem. Soc.* **2003**, *125*, 4964.

[7] J. Okuda, S. Fokken, H.-C. Kang, W. Massa, *Polyhedron* **1998**, *17*, 943; C. R. Cornman, K. M. Geiser-Bush, J. W. Kampf, *Inorg. Chem.* **1999**, *38*, 4303.

[8] R. Siefert, T. Weyhermuller, P. Chaudhuri, *J. Chem. Soc., Dalton Trans.* **2000**, 4656.

[9] T. Miyatake, K. Mizunuma, Y. Seki, M. Kakugo, *Macromol. Chem. Rapid Commun.,* 1989, **10**, 349; T. Miyatake, K. Mizunuma, M. Kakugo, *Macromol. Chem. Macromol. Symp.,* 1993, **66**, 203; F. G. Sernetz, R. Muelhaupt, S. Fokken, J. Okuda, *Macromolecules* **1997**, *30*, 1562; M. Kakugo, T. Miyatake, K. Mizunuma, *Stud. Surf. Sci. Catal.,* 1999, **56**, 517; M. Kakugo, T. Miyatake, K. Mizunuma, Y. Yagi, Sumitomo Chemical Co. U.S. 5043, 408.

[10] R. D. J. Froese, D. G. Musaev, T. Matsubara, K. Morokuma, *J. Am. Chem. Soc.* **1997**, *119*, 7190; R. D. J. Froese, D. G. Musaev, K. Morokuma, *Organometallics* **1999**, *18*, 373.

[11] J. Okuda, E. Masoud, *Macromol. Chem. Phys.* **1998**, *199*, 543.

[12] Y. Takashima, Y. Nakayama, K. Watanabe, T. Itono, N. Ueyama, A. Nakamura, H. Yasuda, A. Harada, *Macromolecules* **2002**, *35*, 7538.

[13] F. G. Sernetz, R. Muelhaupt, S. Fokken, J. Okuda, *Macromolecules* **1997**, *30*, 1562.

[14] W. Kaminsky, *J. Chem. Soc., Dalton Trans.* **1998**, 1413; X. Yan, A. Chernega, M. L. H. Green, J. Sanders, J. Souter, T. Ushioda, *J. Mol. Catal. A: Chem.* **1998**, *128*, 119; G. W. Coates, *Chem. Rev.* **2000**, *100*, 1223.

[15] P. L. Arnold, L. S. Natrajan, J. J. Hall, S. J. Bird, C. Wilson, *J. Organomet. Chem.* **2002**, *647*, 205.

[16] M. C. W. Chan, K.-H. Tam, Y.-L. Pui, N. Zhu, *J. Chem. Soc., Dalton Trans.* **2002**, 3085.

[17] V. Reimer, T. P. Spaniol, J. Okuda, H. Ebeling, A. Tuchbreiter, R. Muelhaupt, *Inorg. Chim. Acta* **2003**, *345*, 221.

[18] J. Okuda, S. Fokken, H.-C. Kang, W. Massa, *Chem. Ber.* **1995**, *128*, 221.

[19] E. Y. Tshuva, I. Goldberg, M. Kol, Z. Goldschmidt, *Inorg. Chem.* **2001**, *40*, 4263.

[20] Y. Nakayama, K. Waatanabe, N. Ueyama, A. Nakamura, A. Harada, J. Okuda, *Organometallics* **2000**, *19*, 2498.

[21] E. Y. Tshuva, I. Goldberg, M. Kol, *Organometallics* **2001**, *20*, 3071; M. G. Thorn, Z. C. Etheridge, P. E. Fanwick, I. P. Rothwell, *J. Organomet. Chem.* **1999**, *591*, 148.

[22] D. W. Stephan, T. T. Nadasdi, *Coord. Chem. Rev.* **1996**, *147*, 147.

[23] A single S−S bond is 1.83 Å; A. Bondi, *J. Phys. Chem.* **1964**, *68*, 441; *International Tables of Crystallography*, Kluwer Academic, Dordrecht, **1992**, vol. C.

[24] W. Nakanishi, S. Hayashi, T. Arai, *Chem. Commun.* **2002**, 2416.

[25] W. Nakanishi, S. Hayashi, S. Toyota, *Chem. Commun.* **1996**, 371; W. Nakanishi, S. Hayashi, S. Toyota, *J. Org. Chem.* **1998**, *63*, 8790; S. Hayashi, W. Nakanishi, *J. Org. Chem.* **1999**, *64*, 6688.

[26] C. Rovira, J. J. Novoa, *Chem. Eur. J.* **1999**, *5*, 3689.

[27] T. N. Guru Row, R. Parthasarathy, *J. Am. Chem. Soc.* **1981**, *103*, 477.

[28] I. Dance, *New. J. Chem.* **2003**, *27*, 22.

[29] S. Fokken, F. Reichwald, T. P. Spaniol, J. Okuda, *J. Organomet. Chem.* **2002**, *663*, 158, for comparison, the activity of the dimethyltitanium complex [(tbmp)TiMe$_2$] towards ethene polymerisation is calculated to be 12.52 kg PE g [Ti]$^{-1}$ bar^{-1} h^{-1}.

[30] M. Bochmann, S. J. Lancaster, M. B. Hursthouse, K. M. Abdul Malik, *Organometallics* **1994**, *13*, 2235; S. J. Lancaster, M. Bochmann, *Organometallics* **1993**, *12*, 663.

[31] F. Guerin, D. H. McConville, J. J. Vittal, G. A. P. Yap, *Organometallics* **1998**, *17*, 5172; R. M. Gauvin, J. Kress, *J. Mol. Catal. A: Chem.* **2002**, *182*/*183*, 411.

[32] For an earlier example of oxygen insertion into a Ti−Me bond, see: G. J. Erskine, G. J. B. Hurst, E. L. Weinberg, B. K. Hunter, J. D. McCowan, *J. Organomet. Chem.* **1984**, *267*, 265.

[33] M. J. Carney, P. J. Walsh, F. J. Hollander, R. G. Bergman, *Organometallics* **1992**, *11*, 761; S. J. Kim, I. N. Jung, B. R. Yoo, S. Cho, J. Ko, S. H. Kim, S. O. Kang, *Organometallics* **2001**, *20*, 1501; J. Scholz, G. A. Hadi, K. H. Thiele, H. Gorls, R. Weimann, H. Schumann, J. Sieler, *J. Organomet. Chem.* **2001**, *626*, 243; Y. Wielstra, S. Gambarotta, A. L. Spek, W. J. J. Smeets, *Organometallics* **1990**, *9*, 2142; H. G. Helmut, C. E. Denner, *J. Organomet. Chem.* **1990**, *391*, 53.

[34] L. S. Natrajan, J. J. Hall, A. J. Blake, C. Wilson, P. L. Arnold, *J. Solid State Chem.* **2003**, *171*, 90.

[35] $TiCl_4\cdot 2thf$ and $ZrCl_4\cdot 2thf$: L. E. Manzer, *Inorg. Synth.* **1985**, *21*, 135; [Zr(CH$_2$Ph)$_4$]: U. Zucchini, E. Albizzati, U. Giannini, *J. Organomet. Chem.* **1971**, 357; [Ti(NMe$_2$)$_4$]: A. A. Naiini, S. L. Ringrose, Y. Su, R. A. Jacobsen, J. G. Verkade, *Inorg. Chem.* **1993**, *32*, 1290; [Zr(NMe$_2$)$_4$]: H. Schreider, G. T. Puchta, F. A. Kaul, G. Raudaschl-Sieber, F. Lefebvre, *J. Mol. Catal. A, Chem.* **2001**, *170*, 127.

[36] P. L. Arnold, J. J. Hall, L. S. Natrajan, A. J. Blake, C. Wilson, *Dalton Trans.* **2003**, 1053.

[37] *SHELXTL 5.10*, Bruker AXS Inc., Madison, Wisconsin, USA, **1997**; G. M. Sheldrick, *Acta Crystallogr., Sect. A* **1990**, *46*, 467. G. M. Sheldrick, *SHELXL-97*, University of Goettingen, Germany, **1997**.

Received February 24, 2004
Early View Article
Published Online July 22, 2004